

# Candidates for the $5\alpha$ condensed state in $^{20}\text{Ne}$

S. Adachi,<sup>1,\*</sup> Y. Fujikawa,<sup>2</sup> T. Kawabata,<sup>1</sup> H. Akimune,<sup>3</sup> T. Doi,<sup>2</sup> T. Furuno,<sup>4</sup> T. Harada,<sup>2</sup>  
K. Inaba,<sup>2</sup> S. Ishida,<sup>5</sup> M. Itoh,<sup>5</sup> C. Iwamoto,<sup>6</sup> N. Kobayashi,<sup>4</sup> Y. Maeda,<sup>7</sup> Y. Matsuda,<sup>5</sup>  
M. Murata,<sup>4</sup> S. Okamoto,<sup>2</sup> A. Sakaue,<sup>8</sup> R. Sekiya,<sup>2</sup> A. Tamii,<sup>4</sup> and M. Tsumura<sup>2</sup>

<sup>1</sup>*Department of Physics, Osaka University, Machikaneyama, Toyonaka, Osaka, Japan 560-0043*

<sup>2</sup>*Department of Physics, Kyoto University, Kitashirakawa-Oiwake, Sakyo, Kyoto 606-8502, Japan*

<sup>3</sup>*Department of Physics, Konan University, Higashinada, Kobe, Hyogo 658-8501, Japan*

<sup>4</sup>*Research Center for Nuclear Physics (RCNP), Osaka University, Ibaraki, Osaka 567-0047, Japan*

<sup>5</sup>*Cyclotron and Radioisotope Center (CYRIC), Tohoku University, Sendai, Miyagi 980-8578, Japan*

<sup>6</sup>*RIKEN Center for Advanced Photonics, RIKEN, Hirosawa, Wako, Saitama 351-0198, Japan*

<sup>7</sup>*Faculty of Engineering, University of Miyazaki, Gakuen-Kibanadai, Miyazaki 889-2192, Japan*

<sup>8</sup>*Nishina Center for Accelerator Based Science, RIKEN, Hirosawa, Wako, Saitama 351-0198, Japan*

(Dated: August 14, 2020)

The alpha-particle condensed state in finite nuclei will shed light on low-density nuclear matter. We carried out the coincidence measurement of  $\alpha$  particles inelastically scattered from  $^{20}\text{Ne}$  at  $0^\circ$  and decay charged particles. We compared the measured excitation-energy spectrum and decay branching ratio with the statistical-decay-model calculations, and found that the newly observed states at  $E_x = 23.6$ , 21.8, and 21.2 MeV in  $^{20}\text{Ne}$  are strongly coupled to a candidate for the  $4\alpha$  condensed state in  $^{16}\text{O}$ . The present result suggests that these states are the candidates for the  $5\alpha$  condensed state in  $^{20}\text{Ne}$ .

The alpha-cluster correlation between two protons and two neutrons is a very important property of atomic nuclei. Because an alpha particle consisting of four nucleons is tightly bound and has no excited state up to 20 MeV, it behaves as a well-established subunit in nuclei. Alpha-clustering phenomena have been studied both from experimental and theoretical sides for a long time, and they are still of great interest. One of the hottest topics is the alpha-particle condensation where alpha clusters are condensed into the same lowest  $0s$  orbit in their common mean field. It is theoretically suggested that this alpha-particle condensation manifests at low densities and temperatures due to the bosonic nature of alpha particles, and this is the Bose-Einstein condensation in the nucleon many-body systems [1].

At lower densities than the nuclear saturation density  $n_0 \approx 0.16 \text{ fm}^{-3}$  and low temperatures, nuclear matter is no longer uniform and the system minimizes its energy by forming clusters such as deuterons, tritons, helium-3s, and alpha particles. The alpha particles, which are the most tightly bound among these clusters, are deposited in nuclear matter below a critical density and form the alpha-particle condensate.

One of the remarkable effects of the alpha-particle condensation is the enhancement of the symmetry energy of nuclear matter. The symmetry energy is conventionally defined as the quadratic coefficient when the internal energy per nucleon of nuclear matter is expanded as the Taylor series of the asymmetry parameter  $\delta = (n_n - n_p)/n_B$ . Here,  $n_n$ ,  $n_p$ , and  $n_B$  denote the number densities of neutrons, protons, and baryons, respectively. The density and temperature dependence of the symmetry energy is of great importance to describe nuclear matter. If the formation of clusters in nuclear

matter is taken into account, the internal energies per nucleon are considerably lowered around  $\delta = 0$  particularly at low temperatures. Therefore, the symmetry energy as the curvature of the internal energy with respect to  $\delta$  substantially increases at low densities below  $n_B \sim 10^{-2} \text{ fm}^{-3}$  [2–4]. The equation of state (EoS) of nuclear matter is hence influenced by the alpha-particle condensation. Construction of the EoS is one of the ultimate goals in nuclear physics not only because it is the benchmark of our understanding about strongly interacting fermions but also because it is required to describe many astrophysical phenomena such as neutron stars, supernovae, and the nucleosynthesis in the universe.

The alpha-particle condensation is expected to manifest in finite nuclei as well as in nuclear matter. It should be noted that the alpha-particle condensation can be experimentally studied only in finite nuclei because nuclear matter is nothing but imaginary substance on the earth. The properties of the alpha-particle condensed states (ACSs) such as energies and widths will shed light on low-density nuclear matter.

The authors of Refs. [1, 5] proposed the Tohsaki-Horiuchi-Schuck-Röpke (THSR) wave function to describe the  $0^+$  states in  $^8\text{Be}$ ,  $^{12}\text{C}$ , and  $^{16}\text{O}$ , and theoretically suggested the ACSs emerge near the  $2\alpha$ ,  $3\alpha$ , and  $4\alpha$ -decay threshold energies, respectively. The THSR wave function demonstrates that these states are low-density states composed of weakly interacting alpha particles condensed into the lowest  $0s$  orbit, and are akin to the alpha-particle condensate in nuclear matter. The following work [6] predicted that similar ACSs should exist slightly above  $k\alpha$ -decay thresholds in heavier self-conjugate  $A = 4k$  nuclei up to  $k \sim 10$ , however, the experimental information on the ACSs was obtained in

limited nuclei so far.

Let us briefly describe the present situation on the ACSs in the self-conjugate  $A = 4k$  nuclei. The ground state of  ${}^8\text{Be}$  and the  $0_2^+$  state in  ${}^{12}\text{C}$  locate near the  $2\alpha$  and  $3\alpha$ -decay thresholds and are nicely described with the spatially developed wave functions by the fully microscopic alpha-cluster models [5, 7, 8]. These wave functions reasonably well reproduce the energies and inelastic form factors of these states, and are almost equivalent to the THSR wave functions for the  $2\alpha$  and  $3\alpha$  condensed states [5, 9]. These facts are the strong evidence that the ground state of  ${}^8\text{Be}$  and the  $0_2^+$  state in  ${}^{12}\text{C}$  are the ACSs.

The ACS in  ${}^{16}\text{O}$  was theoretically predicted to be the  $0_6^+$  state [10, 11]. The corresponding state was observed in many reactions at  $E_x = 15.097 \pm 0.005$  MeV with the width of  $166 \pm 30$  keV [12]. Recently the authors of Ref. [13] found that this state decays into the  ${}^8\text{Be}(0_1^+) + {}^8\text{Be}(0_1^+)$  or  ${}^{12}\text{C}(0_2^+) + \alpha$  channel with the almost same probabilities. The  $0_6^+$  state in  ${}^{16}\text{O}$  is therefore highly probable to be the ACS.

For  ${}^{20}\text{Ne}$  and heavier nuclei, no known states are assigned to the ACSs. Only a tentative candidate for the  $5\alpha$  condensed state was experimentally proposed. The several  $0^+$  states observed in the  ${}^{22}\text{Ne}(p, t){}^{20}\text{Ne}$  reaction were examined with the shell-model calculation [14]. It was found that one of the  $0^+$  states at  $E_x = 22.5$  MeV was not described by the shell model, and its excitation energy is close to  $E_x = 21.14$  MeV where the  $5\alpha$  condensed state is predicted in Ref. [6]. However, the excitation energy is not conclusive evidence for the ACS because many  $0^+$  states exist around the expected excitation energy. Further information is necessary to identify the ACS. It should be noted that the decay property of the excited state provides additional information. Considering the nature of ACSs, an overlap between wave functions of ACSs in different nuclei should be large. Therefore, ACSs should prefer to decay via ACSs in lighter nuclei by emitting alpha particles. Because energy differences between ACSs are smaller than a few MeV [6], emission of low-energy  $\alpha$  particles from  $0^+$  states near  $k\alpha$ -decay thresholds can be a clue to identify ACSs.

It is worthy to mention the recent measurement of the  ${}^{12}\text{C}({}^{16}\text{O}, {}^{28}\text{Si}^*)$  reaction [15]. Decay alpha particles were comprehensively detected to obtain the invariant-mass spectra of  ${}^{16}\text{O}$ ,  ${}^{20}\text{Ne}$ , and  ${}^{24}\text{Mg}$ , but no ACSs were found. The authors claimed that the Coulomb barrier inherently suppresses low-energy-particle decays and obscures the signature of the ACSs. However, some of the authors previously pointed out that the Coulomb barrier in the ACSs should be suppressed due to their dilute nature [16]. One of plausible explanations for this contradictory situation is that the ACSs were hidden by a lot of backgrounds from various high-spin states in Ref. [15] because large angular momenta were brought to the sys-

tem in the heavy-ion collision. Since ACSs have the spin and parity of  $0^+$  and isospin of 0, nuclear reactions which selectively excite isoscalar  $0^+$  states should be employed to populate ACSs. One of the best reactions to populate isoscalar  $0^+$  states is inelastic alpha scattering at forward angles [17]. Because both the spin and isospin of the alpha particle are 0, the inelastic alpha scattering off self-conjugate  $A = 4k$  nuclei selectively excites isoscalar natural-parity states. In addition, the cross sections for the  $0^+$  states have their maximum at  $0^\circ$ .

In the present work, we carried out the coincidence measurement of alpha particles inelastically scattered from  ${}^{20}\text{Ne}$  at  $0^\circ$  and decay charged particles emitted from excited states in order to search for the  $5\alpha$  condensed state in  ${}^{20}\text{Ne}$ . The experiment was conducted at the Research Center for Nuclear Physics (RCNP), Osaka University. The experimental setup was almost same with Ref. [18] except a  ${}^{20}\text{Ne}$  gas target and a Si telescope array.

A 386-MeV  ${}^4\text{He}^{2+}$  beam with an intensity of about 10 nA was transported to an isotopically enriched  ${}^{20}\text{Ne}$  gas target. The  ${}^{20}\text{Ne}$  gas was filled in the target cell at 14.1 kPa and at room temperature, and sealed with the 100 nm-thick silicon nitride ( $\text{SiN}_x$ ) membranes as the entrance and exit windows. The thickness of the target cell along the beam axis was 8.0 mm, which corresponds to the mass thickness of  $89.6 \mu\text{g}/\text{cm}^2$  of the  ${}^{20}\text{Ne}$  gas. In order to identify the ACS decaying into the  $4\alpha$  condensed state in  ${}^{16}\text{O}$ , it was required to detect the decay alpha particles whose energies are lower than a few MeV. The thin  $\text{SiN}_x$  membrane enabled low-energy alpha particles down to  $E = 0.04$  MeV to escape from the target cell. The pressure and temperature of the  ${}^{20}\text{Ne}$  gas were monitored using the diaphragm gauge and the platinum resistor during the measurement. The backgrounds from the  $\text{SiN}_x$  membranes were subtracted by using the measurement with the empty cell. We found that background events due to  ${}^{\text{nat}}\text{C}$  increased with the measurement time. It was supposed that oil mists from the vacuum pumps were baked by the beam and deposited on the surface of the target cell. These backgrounds were also successfully subtracted by using the measurement with  ${}^{\text{nat}}\text{C}$  foil.

In order to detect decay particles from excited states in  ${}^{20}\text{Ne}$ , we installed a Si telescope array around the target covering  $0.42$  sr (3.4% of  $4\pi$ ) at  $\theta_{\text{lab}} = 106.4\text{--}163.0^\circ$ . The Si telescope array consisted of six segments. The distance between each segment and the target was 170 mm. Each segment had three layers of Si detectors, but only the first and second layers were used in the present analysis. The thicknesses of the first and second layers were  $65 \mu\text{m}$  and  $500 \mu\text{m}$  in order from the target side, and their dimensions were  $50 \text{ mm} \times 50 \text{ mm}$ . The first layers were divided into 8 strips and the second layers were read as a single pad. The first Si detectors had the dead layer with the thickness of about  $1.2 \mu\text{m}$  on the rear side.

Particle identification for decay particles which pene-

trated the first layer was performed by using the correlation between the energy loss in the first layer and the total energy, whereas for low-energy particles which could not penetrate the first layer, the time of flight from the target to the Si detector and the total energy were used.

Figure 1 shows the correlation between the kinetic energies of decay alpha particles ( $K_\alpha$ ) and the excitation energies of  $^{20}\text{Ne}$  [ $E_x(^{20}\text{Ne})$ ]. Linear loci corresponding to

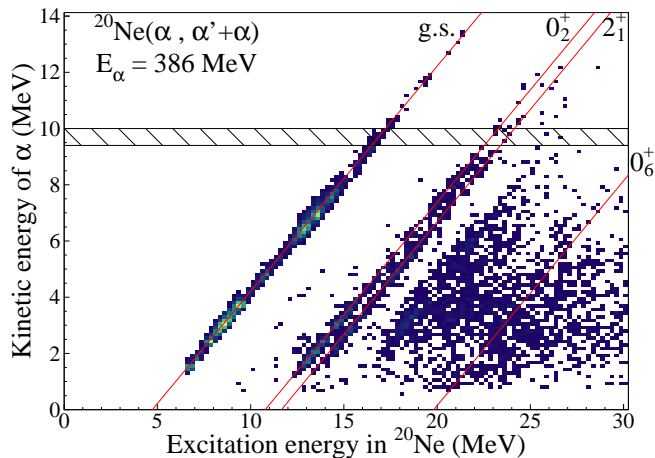


FIG. 1. Correlation between the kinetic energy of decay alpha particles and the excitation energies of  $^{20}\text{Ne}$ . The red solid lines indicate the calculated correlation in the  $\alpha$ -decay events into the ground,  $0_2^+$ ,  $2_1^+$ , and  $0_6^+$  states in  $^{16}\text{O}$ . The experimental data in the hatched area are accompanied by uncertainties on the kinetic energies of alpha particles due to dead layers of the Si detectors.

the  $\alpha$ -decay events into the ground,  $0_2^+$ , and  $2_1^+$  states in  $^{16}\text{O}$  are clearly seen. In the two-body decay of  $^{20}\text{Ne}$  into the  $^{16}\text{O} + \alpha$  channel,  $K_\alpha$  correlates with  $E_x(^{20}\text{Ne})$  via the excitation energy of  $^{16}\text{O}$  [ $E_x(^{16}\text{O})$ ] as  $K_\alpha = m_{^{16}\text{O}}/(m_{^{16}\text{O}} + m_\alpha)[E_x(^{20}\text{Ne}) - E_{\text{th}}(^{16}\text{O} + \alpha) - E_x(^{16}\text{O})]$ .  $E_{\text{th}}(^{16}\text{O} + \alpha)$  is the threshold energy for the  $^{16}\text{O} + \alpha$  decay in  $^{20}\text{Ne}$ , and  $m_{^{16}\text{O}(\alpha)}$  is the rest mass of  $^{16}\text{O}$  (the  $\alpha$  particle).

Figure 2(a) shows the excitation-energy spectrum of the  $^{20}\text{Ne}(\alpha, \alpha')$  reaction at  $0^\circ$  for the singles events obtained by measuring inelastically scattered alpha particles only. No clear peaks are observed around a few MeV above the  $5\alpha$  decay threshold where the ACS is expected. Figure 2(b) shows the excitation-energy spectrum for the coincidence events in which one alpha particle was detected by the Si telescope array. The obtained yield was converted to the cross section on the basis of the fact that the  $\alpha$ -decay probability of the  $0_2^+$  state at  $E_x = 6.73$  MeV in  $^{20}\text{Ne}$  is almost 100%. Note that the cross sections for the  $^{20}\text{Ne}(\alpha, \alpha' + \alpha)$  reaction in Fig. 2(b) can be apparently larger than those for the  $^{20}\text{Ne}(\alpha, \alpha')$  reaction in Fig. 2(a) above the  $^{12}\text{C} + 2\alpha$  threshold because more than one alpha particle are emitted. It is remarkable that the two narrow peaks are observed at  $E_x = 23.6$  and  $21.8$  MeV

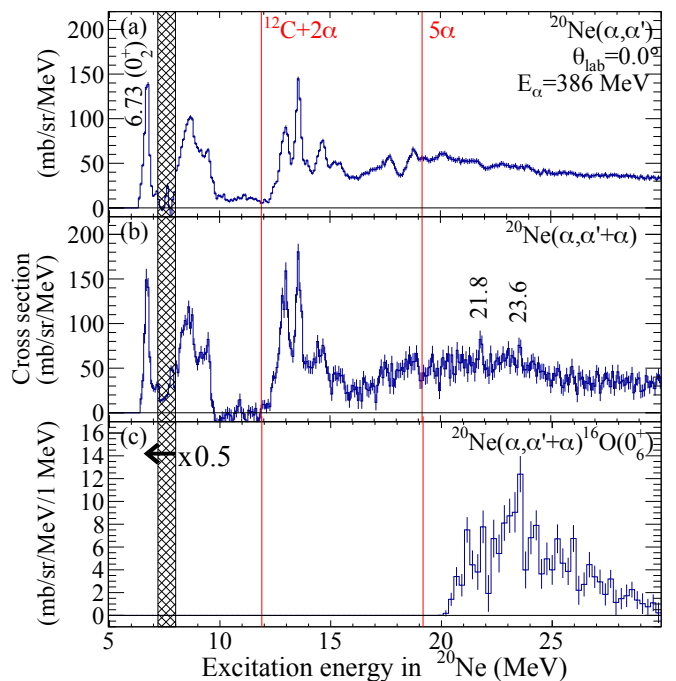


FIG. 2. Excitation-energy spectra of the  $^{20}\text{Ne}(\alpha, \alpha')$  reaction at  $0^\circ$  for (a) the singles events and (b) the coincidence events. (c) Same as (b) but when the  $E_x(^{16}\text{O})$  is close to the excitation energy of the  $0_6^+$  state. The spectra at  $E_x < 8.0$  MeV are downscaled by a factor of 0.5. The vertical lines at  $E_x = 11.9$  and  $19.2$  MeV represent the  $^{12}\text{C} + 2\alpha$  and  $5\alpha$  decay thresholds. The hatched area indicates the excitation-energy region where a strong peak due to the  $0_2^+$  state in the  $^{12}\text{C}$  contaminants caused large errors in the background subtraction.

above the  $5\alpha$  decay threshold although their statistical significance is not fully high.

In order to search for the  $5\alpha$  condensed state, we focused on the  $\alpha$ -decay events into the  $0_6^+$  state in  $^{16}\text{O}$  because this state is a strong candidate for the  $4\alpha$  condensed state. We reconstructed  $E_x(^{16}\text{O})$  from  $K_\alpha$  and  $E_x(^{20}\text{Ne})$  assuming the two-body  $^{20}\text{Ne}^* \rightarrow ^{16}\text{O} + \alpha$  decay, and selected the events at  $E_x(^{16}\text{O}) = 15.1 \pm 0.5$  MeV as shown in Fig. 2(c). The same normalization factor with Fig. 2(b) was used to convert the yield to the cross section.

The excitation-energy spectrum in Fig. 2(c) was compared with the theoretical spectrum calculated by the statistical-decay model in Fig. 3. This model takes into account the spins, parities, isospins, energies and level densities of the mother and its descendant nuclei as well as transmission coefficients for decay particles. Decay branching ratios of excited states in  $^{20}\text{Ne}$  into particle- ( $\alpha$ ,  $p$ , and  $n$ ) and  $\gamma$ -decay channels were calculated with the computer code CASCADE [19] assuming that the initial excited state is the isoscalar state with its spin and parity of  $0^+$ ,  $1^-$ , or  $2^+$ . Using the theoretical branching ratios, we performed the Monte Carlo calculation to simulate the decay processes of the excited states in  $^{20}\text{Ne}$ .

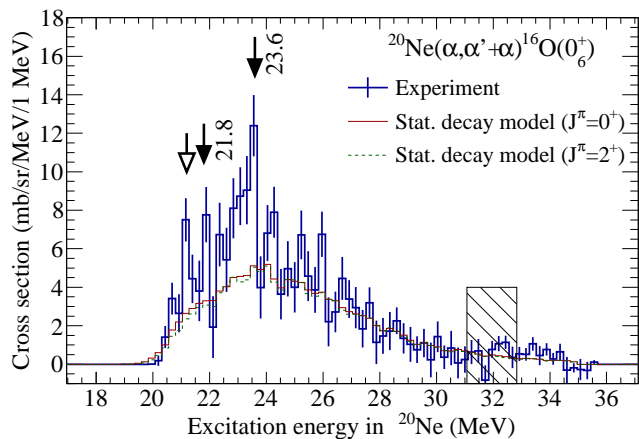


FIG. 3. Same excitation-energy spectrum as Fig. 2(c) (thick solid lines with error bars) compared with the statistical-decay-model calculations for the  $0^+$  and  $2^+$  states in  $^{20}\text{Ne}$  (thin red solid and green dashed lines). Uncertainties on the kinetic energies of alpha particles due to dead layers of the Si detectors are accompanied in the hatched area as in Fig. 1.

The decay processes were traced until all of the descendant nuclei settled in their ground states under the assumption that decay particles were emitted isotropically in the rest frame of the decaying nuclei. The simulated decay events were analyzed in the same manner with the experimental data after the energies of decay particles were randomly varied according to the experimental resolution of 0.40 MeV at the full width at half maximum. The theoretical spectra for the  $0^+$ ,  $1^-$ , and  $2^+$  states were almost the same. Therefore, only the theoretical spectra for the  $0^+$  and  $2^+$  states are presented in Fig. 3. The theoretical spectra were multiplied by a factor of 0.59 to fit the experimental spectrum between  $E_x = 27$  and 31 MeV where no structures were observed in the experimental spectrum. In contrast to the good agreement between the theoretical calculations and the experiment above  $E_x = 25$  MeV, the noticeable excesses of the experimental cross sections from the calculations were found in the vicinities of  $E_x = 23.6$  and 21.8 MeV indicated by the solid arrows where the narrow peaks are observed in Fig. 2(b). The experimental cross section also exceeds the calculations at  $E_x = 21.2$  MeV, which is closer to the  $5\alpha$  threshold than the two states at  $E_x = 23.6$  and 21.8 MeV, as indicated by the open arrow.

In order to examine the decay properties of the new state at  $E_x = 23.6$  MeV in  $^{20}\text{Ne}$ , the  $\alpha$ -decay events at  $E_x = 23.6 \pm 0.24$  MeV were selected, and the decay branching ratio into  $^{16}\text{O}$  was obtained assuming the two-body decay as shown in Fig. 4. The theoretical branching ratios of the isoscalar  $0^+$  and  $2^+$  states at the same excitation energy ( $E_x = 23.6 \pm 0.24$  MeV) were obtained from the simulated decay events using the same normalization factor as in Fig. 3, and compared with the experiment as presented by the thin red solid and green dashed lines.

The theoretical branching ratios do not change much de-

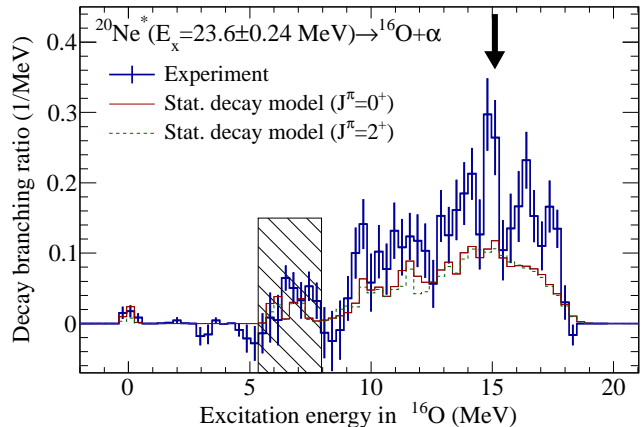


FIG. 4. Decay branching ratio of the excited state in  $^{20}\text{Ne}$  at  $E_x = 23.6 \pm 0.24$  MeV populated by the inelastic alpha scattering at  $0^\circ$  (thick blue solid lines with error bars) compared with the statistical-decay-model calculations from the isoscalar  $0^+$  and  $2^+$  states in  $^{20}\text{Ne}$  (thin red solid and green dashed lines). Uncertainties on the kinetic energies of alpha particles due to dead layers of the Si detectors are accompanied in the hatched area as in Fig. 1.

pending on the spin of the initial excited states. Several prominent peaks were observed on the continuous spectrum calculated by the statistical-decay model. It should be noted that the location of the strongest peak around  $E_x(^{16}\text{O}) = 15$  MeV agrees with that of the  $0_6^+$  state in  $^{16}\text{O}$  at  $E_x(^{16}\text{O}) = 15.1$  MeV indicated by the vertical arrow.

It was desirable to examine the decay properties of the excited states at  $E_x = 21.8$  and 21.2 MeV in  $^{20}\text{Ne}$  as well as at  $E_x = 23.6$  MeV, however the experimental statistics was too poor to compare them with the theoretical calculations.

Figures 3 and 4 show that the newly found excited state at  $E_x = 23.6$  MeV is strongly coupled to the  $0_6^+$  state in  $^{16}\text{O}$  which is a candidate for the  $4\alpha$  condensed state. This 23.6-MeV state is a candidate for the  $5\alpha$  condensed state. However, the measured excitation energy is considerably higher than the theoretical value of  $E_x = 21.14$  MeV [6]. This might suggest another interpretation that either of the low-energy states at  $E_x = 21.8$  or 21.2 MeV corresponds to the  $5\alpha$  condensed state, and the 23.6-MeV state is akin to the  $5\alpha$  condensed state like the  $2_2^+$  state in  $^{12}\text{C}$ , which is an excited state of the relative motion of alpha clusters in the  $3\alpha$  condensed state [8, 20–22]. In order to clarify the correspondence between these new states and the  $5\alpha$  condensed state, it is necessary to determine their spins and parities. However, the spins and parities of the new states are still unknown because we did not measure the angular distribution of the cross sections in the present work. An additional measurement is therefore strongly desired.

In summary, we carried out the coincidence measurement of alpha particles inelastically scattered from  $^{20}\text{Ne}$  at  $0^\circ$  and decay charged particles from excited states in order to search for the  $5\alpha$  condensed state in  $^{20}\text{Ne}$ . Comparing the measured excitation-energy spectrum and decay branching ratio with the statistical-decay-model calculation, we found that the newly observed states at  $E_x = 23.6, 21.8,$  and  $21.2$  MeV in  $^{20}\text{Ne}$  are strongly coupled to the  $0_6^+$  state in  $^{16}\text{O}$ . These states are the candidates for the  $5\alpha$  condensed state in  $^{20}\text{Ne}$  because the  $0_6^+$  state in  $^{16}\text{O}$  is a strong candidate for the  $4\alpha$  condensed state. However, their spins and parities are still unknown. An additional measurement to determine their spins and parities is strongly desired.

The authors acknowledge the RCNP cyclotron crews for providing a high-quality beam for background-free measurements at  $0^\circ$ . This work was performed under the RCNP E402 program, and partly supported by JSPS KAKENHI Grants No. JP20K14490, JP19J20784, and JP19H05153.

---

\* [adachi@ne.phys.sci.osaka-u.ac.jp](mailto:adachi@ne.phys.sci.osaka-u.ac.jp)

- [1] A. Tohsaki, H. Horiuchi, P. Schuck, and G. Röpke, *Phys. Rev. Lett.* **87**, 192501 (2001).
- [2] S. Typel, G. Röpke, T. Klähn, D. Blaschke, and H. H. Wolter, *Phys. Rev. C* **81**, 015803 (2010).
- [3] S. Typel, H. H. Wolter, G. Röpke, and D. Blaschke, *Eur. Phys. J. A* **50**, 17 (2014).
- [4] Z. W. Zhang and L. W. Chen, *Phys. Rev. C* **100**, 054304 (2019).
- [5] Y. Funaki, H. Horiuchi, A. Tohsaki, P. Schuck, and G. Röpke, *Prog. Theo. Phys.* **108**, 297 (2002).
- [6] T. Yamada and P. Schuck, *Phys. Rev. C* **69**, 024309 (2004).
- [7] R. B. Wiringa, S. C. Pieper, J. Carlson, and V. R. Pandharipande, *Phys. Rev. C* **62**, 014001 (2000).
- [8] M. Kamimura, *Nucl. Phys. A* **351**, 456 (1981).
- [9] Y. Funaki, A. Tohsaki, H. Horiuchi, P. Schuck, and G. Röpke, *Phys. Rev. C* **67**, 051306(R) (2003).
- [10] Y. Funaki, T. Yamada, H. Horiuchi, G. Röpke, P. Schuck, and a. Tohsaki, *Phys. Rev. Lett.* **101**, 082502 (2008).
- [11] Y. Funaki, *Phys. Rev. C* **97**, 021304 (2018).
- [12] D. R. Tilley, H. R. Weller, and C. M. Chevesyc, *Nucl. Phys. A* **565**, 1 (1993).
- [13] M. Barbui, K. Hagel, J. Gauthier, S. Wuenschel, R. Wada, V. Z. Goldberg, R. T. DeSouza, S. Hudan, D. Fang, X. G. Cao, and J. B. Natowitz, *Phys. Rev. C* **98**, 044601 (2018).
- [14] J. A. Swartz, B. A. Brown, P. Papka, F. D. Smit, R. Neveling, E. Z. Buthelezi, S. V. Förtsch, M. Freer, T. Kokalova, J. P. Mira, F. Nemulodi, J. N. Orce, W. A. Richter, and G. F. Steyn, *Phys. Rev. C* **91**, 034317 (2015).
- [15] J. Bishop, T. Kokalova, M. Freer, L. Acosta, M. Assié, S. Bailey, G. Cardella, N. Curtis, E. D. Filippo, D. D. Aquila, S. D. Luca, L. Francalanza, B. Gnoffo, G. Lanzalone, I. Lombardo, N. S. Martorana, S. Norella, A. Pagano, E. V. Pagano, M. Papa, S. Pirrone, G. Politi, F. Rizzo, P. Russotto, L. Quattrocchi, R. Smith, I. Stefan, A. Trifirò, M. Trimarchi, G. Verde, M. Vigilante, and C. Wheldon, *Phys. Rev. C* **100**, 034320 (2019).
- [16] T. Kokalova, N. Itagaki, W. Von Oertzen, and C. Wheldon, *Phys. Rev. Lett.* **96**, 192502 (2006).
- [17] M. N. Harakeh and A. v. d. Woude, *Giant Resonance: Fundamental High-Frequency Modes of Nuclear Excitation* (Oxford University Press, 2001).
- [18] M. Itoh, H. Sakaguchi, M. Uchida, T. Ishikawa, T. Kawabata, T. Murakami, H. Takeda, T. Taki, S. Terashima, N. Tsukahara, Y. Yasuda, M. Yosoi, U. Garg, M. Heden, B. Kharraja, M. Koss, B. K. Nayak, S. Zhu, H. Fujimura, M. Fujiwara, K. Hara, H. P. Yoshida, H. Akimune, M. N. Harakeh, and M. Volkerts, *Phys. Rev. C* **68**, 064602 (2003).
- [19] F. Pühlhofer, *Nucl. Phys. A* **280**, 267 (1977).
- [20] E. Uegaki, Y. Abe, S. Okabe, and H. Tanaka, *Prog. Theor. Phys.* **57**, 1262 (1979).
- [21] P. Descouvemont and D. Baye, *Phys. Rev. C* **36**, 54 (1987).
- [22] Y. Funaki, *Phys. Rev. C* **92**, 021302(R) (2015).